Structured sparsity regularization for gravitational-wave polarization reconstruction

Fangchen Feng, Eric Chassande-Mottin and Philippe Bacon
APC, Univ. Paris Diderot, CNRS/IN2P3
CEA/Irfu, Obs. de Paris, Sorbonne Paris Cité
75205 Paris, France

Aurélia Fraysse
Laboratoire des signaux et systèmes
CNRS, CentraleSupélec, Univ. Paris-Sud, France

***Abstract*—Gravitational-wave (GW) observations with a network of more than two advanced detectors open the possibility of reconstructing the two polarizations predicted by General Relativity. We propose to address this problem using sparsity promoting regularizations. We consider a variety of techniques, including "structured sparsity" that allows to explicitly model the intrinsic clustering effect occurring in the time-frequency representation of GW transient signals. The proposed methods are evaluated with simulated GW signals and real-world noise. Numerical simulations show the advantages of the proposed approaches.**

I. Introduction

Gravitational-wave (GW) observations offer new perspectives in astronomy [1], giving access to objects such as black-hole binaries that were hidden to more conventional observatories. The network of advanced detectors initiated by Advanced LIGO, recently joined by Advanced Virgo will expand in the next future with the detector Kagra in Japan and LIGO-India. More detectors mean more sensitive combined observations that allow reaching more distant sources, better sky coverage, and better resolution of the source position in the sky. This also allows better constraints on the two GW polarizations denoted h_+ and $h_\times$, predicted by General Relativity, which opens the possibility of new tests for this fundamental theory of gravity and to infer non-standard effects occurring in the source dynamics, such as the precession of the compact binary orbital plane [2].

Each detector receives a linear combination of the two polarizations. Therefore, reconstructing GW polarizations from the observations is an inverse problem, that can be ill-posed [3]–[5]. Coherent data analysis techniques allow estimating the *detector response* i.e., the GW signal received by each detector. These include the likelihood-based search algorithm *coherent Waveburst* [6] and the Bayesian algorithm *Bayeswave* [7]. So far, there are only a limited number of studies such as [8] about the estimation of the polarizations rather the detector responses. This is the main topic of interest in this proceeding.

Regularization is a key ingredient in the resolution of inverse problems [9]. Here, we investigate the potential of sparsity promoting priors [10] to regularize the inversion. The motivation is that the transient GW can be well described by few bright outlier pixels in a time-frequency transform, therefore a sparse time-frequency representation. Sparsity regularization has been previously studied in the context of GW burst searches in [11], [12] and in this paper, we introduce new polarization reconstruction algorithms that use sparsity regularization, and compare the reconstruction error to the one obtained with other approaches.

In Sec II, we formulate the reconstruction problem. Sec III introduces the considered reconstruction methods. Numerical evaluation is performed in Sec IV and Sec V concludes the paper.

II. Formulation of the problem

According to General Relativity, GWs possess by two independent polarizations h_+ and $h_\times$. Detectors measure a linear combination of those two polarizations. The signal received by the k-th detector in the observing network can be expressed as [1]:

$$x_k(t) = \mathbf{f}_k^T \mathbf{h}(t - \tau_k) + n_k(t), \tag{1}$$

where $\mathbf{f}_k = [F_{k+}, F_{k\times}]^T$ is the antenna response of the considered detector to the polarizations $\mathbf{h} = [h_+, h_\times]^T$. Here, τ_k denotes the delay in the arrival time at the detector location relative to the Earth center taken as the reference location. In (1), both $\mathbf{f}_k$ and τ_k are known functions of the source sky direction. GW observations are limited by an additive background noise $n_k(t)$ which is assumed to be Gaussian and (locally) stationary with power spectral density $S_k(f)$. We assume that the source sky direction is *known*, so that the beam pattern $\mathbf{f}_k$ and the delay τ_k are fixed. This allows to simplify the problem and concentrate on the effect of signal regularization, the focus of this article. This assumption also corresponds to the practical case where the position of the source is obtained by other (non-GW) observables (see e.g., [13]).

With no loss of generality, the observation of the detector network can now be written as:

$$\mathbf{x}(t) = \mathcal{F}\mathbf{h}(t) + \mathbf{n}(t), \tag{2}$$

where $\mathbf{x} = [x_1, \ldots, x_K]^T$, $\mathbf{n} = [n_1, \ldots, n_K]^T$ and the (known) beam pattern matrix $\mathcal{F} = \left[\mathbf{f}_1^T, \ldots, \mathbf{f}_K^T\right]^T$. The goal of the polarization reconstruction problem is to estimate $\mathbf{h}(t)$ from the noisy observations $\mathbf{x}(t)$.

ISBN 978-90-827970-1-5

We map the data to the time-frequency domain using the short-time Fourier transform (STFT) by LTFAT package [14]. In our simulation, we used a Hann window of length 125 ms with 87.5% overlap). We denote $x_k(f,\tau)$ the STFT coefficients of $x_k(t)$.

We assume that the noise power spectral density $S_k(f)$ can be estimated from a stretch of noise-only data; so that whitened observations can be produced directly in the time-frequency domain with $\tilde{x}_k(f,\tau) = x_k(f,\tau)/\sqrt{S_k(f)}$.

The observation equation (2) becomes:

$$\tilde{\mathbf{x}}(f,\tau) = \tilde{\mathcal{F}}(f)\mathbf{h}(f,\tau) + \tilde{\mathbf{n}}(f,\tau), \tag{3}$$

where $\tilde{\mathbf{x}}(f,\tau) = [\tilde{x}_1(f,\tau),\ldots]^T$ collects the whitened observations, $\tilde{\mathcal{F}}(f) = \left[\mathbf{f}_1^T/\sqrt{S_1(f)},\ldots\right]^T$ is the noise-scaled beam pattern matrix and $\mathbf{h}(f,\tau)$ and $\tilde{\mathbf{n}}(f,\tau)$ are respectively the STFT coefficients of $\mathbf{h}(t)$ and whitened noise $\tilde{\mathbf{n}}(t)$. By stacking coefficients obtained at given frequency f for different times into matrices Eq. (3) can be conveniently re-expressed as:

$$\tilde{\mathbf{X}}_f = \tilde{\mathcal{F}}(f)\mathbf{H}_f + \tilde{\mathbf{N}}_f, \tag{4}$$

where $\tilde{\mathbf{X}}_f \in \mathbb{C}^{K\times T}$, $\mathbf{H}_f \in \mathbb{C}^{2\times T}$ and $\tilde{\mathbf{N}}_f \in \mathbb{C}^{K\times T}$ with T, the number of time bins in the STFT transform. In this formulation, the goal is to estimate $\mathbf{H}_f$ from $\tilde{\mathbf{X}}_f$ at each frequency f.

III. Resolving the inverse problem

We now review the reconstruction methods we consider in this article.

A. Truncated least-square inversion

The search algorithm in [15] identifies a set of "bright" time-frequency coefficients with an energy $E(f,\tau) = \sum_k \tilde{x}_k^2(f,\tau)$ above a threshold η, defined from the detector noise level. Inspired by this approach and based on the observation equation (3), the *truncated least square* (TLS) inversion reads

$$\min_{\mathbf{h}(f,\tau)} \sum_{E(f,\tau)>\eta} \|\tilde{\mathbf{x}}(f,\tau) - \tilde{\mathcal{F}}(f)\mathbf{h}(f,\tau)\|_2^2. \tag{5}$$

The above minimization can be solved explicitly by:

$$\mathbf{h}^{\text{TLS}}(f,\tau) = [\tilde{\mathcal{F}}(f)^T\tilde{\mathcal{F}}(f)]^{-1}\tilde{\mathcal{F}}(f)^T\tilde{\mathbf{x}}(f,\tau), \tag{6}$$

for all selected pixels, and zero otherwise.

B. Inversion with ℓ_1 sparsity regularization

GW transients are expected to be sparse in the time-frequency domain. We propose to use this property to regularize the reconstruction of the polarizations. The ℓ_1 norm is often used as a penalty for the sparsity [16]. From (4), the reconstruction with this penalization reads:

$$\min_{\tilde{\mathbf{H}}_f} Q(\mathbf{H}_f) + \lambda_f\|\mathbf{H}_f\|_1, \tag{7}$$

where $Q(\mathbf{H}_f) \equiv \frac{1}{2}\|\tilde{\mathbf{X}}_f - \tilde{\mathcal{F}}(f)\mathbf{H}_f\|_F^2$ and λ_f is a hyperparameter that balances the data fidelity and the regularization. $\|\cdot\|_F$ is the Frobenius norm of a matrix. Note that (7) is frequency-wise. In statistics, this problem and related algorithm is referred to as *Lasso* [17].

The problem (7) can be tackled using the proximal-based algorithm [18]. We recall that the proximal operator which corresponds to the ℓ_1 norm is the entry-wise soft-thresholding:

$$\mathcal{S}_{\lambda_f}(\mathbf{H}_f) : \hat{h}_{j,f} = h_{j,f}(1 - \lambda_f/|h_{j,f}|)^+, \tag{8}$$

where $h_{j,f}$ is the j-th element of $\mathbf{H}_f$ and $(h)^+ \equiv \max(0,h)$.

The algorithm is given in Algorithm 1. The Lipschitz constant of $\nabla Q(\tilde{\mathbf{H}}_f)$ is $L_f = \|\tilde{\mathcal{F}}(f)^T\tilde{\mathcal{F}}(f)\|_2$ where $\|\cdot\|_2$ denotes the spectral norm of a matrix.

Algorithm 1: Lasso

Initialisation : $\mathbf{H}_f^{(1)} \in \mathbb{C}^{2\times T}$, $i = 1$;
repeat
  $\nabla Q(\mathbf{H}_f^{(i)}) = -\tilde{\mathcal{F}}^T(f)\left(\tilde{\mathbf{X}}_f - \tilde{\mathcal{F}}(f)\mathbf{H}_f^{(i)}\right)$;
  $\mathbf{H}_f^{(i+1)} = \mathcal{S}_{\lambda_f/L_f}\left(\mathbf{H}_f^{(i)} - \nabla Q(\mathbf{H}_f^{(i)})/L_f\right)$;
  $i = i + 1$;
until *convergence*;

C. Inversion with structured sparsity

The sparsity penalty considered in the previous section corresponds to a Bayesian prior where all time-frequency coefficients are drawn independently. This ignores the time-frequency structure expected in transient GW signals: the signal power typically accumulates in clusters in the time-frequency domain. To include this effect in our model, we consider the structured sparsity penalty known as *Windowed-Group-Lasso* (WGL). This type of penalty has been applied with success for audio declipping [19] and source separation [20].

The WGL operator replaces the soft-thresholding operator in (8) by:

$$\mathcal{S}_{\lambda_f}^{\text{WGL}}(\mathbf{H}_f) : \hat{h}_{j,f} = h_{j,f}(1 - \lambda_f/h_{j,f}^{(w)})^+, \tag{9}$$

where

$$h_{j,f}^{(w)} = \left(\sum_{j'\in\mathcal{N}_{j,f}} w_{j',f}^{(j,f)}|h_{j',f}|^2\right)^{1/2} \tag{10}$$

with $\mathcal{N}_{j,f}$, the neighborhood of point (j,f) associated with weights $w_{j',f}^{(j,f)}$. This operator corresponds to a convex regularizer involving a mixed norm [21].

The mechanism of this shrinkage operator is to select a coefficient if the energy in its neighborhood is sufficiently large. Consequently, isolated large coefficients tends to be discarded, while small coefficients in the middle of larger ones are kept [21]. The neighborhood, as well as the weights, is usually pre-defined based on the morphological property of the considered signals. Different forms of neighborhood promote different clustering effects. Although the observation equations are formulated for a fixed frequencies, neighborhoods across

ISBN 978-90-827970-1-5 © EURASIP 2018

covering different frequencies can nonetheless be chosen to promote clustering along the frequency direction as well. The corresponding algorithm is shown in Algorithm 2.

Algorithm 2: WGL

Initialisation : $\mathbf{H}_f^{(1)} \in \mathbb{C}^{2\times T}$, $i = 1$;
repeat
  $\nabla Q(\mathbf{H}_f^{(i)}) = -\tilde{\mathcal{F}}^T(f)\left(\tilde{\mathbf{X}}_f - \tilde{\mathcal{F}}(f)\mathbf{H}_f^{(i)}\right)$;
  $\mathbf{H}_f^{(i+1)} = \mathcal{S}^{\text{WGL}}_{\lambda_f/L_f}\left(\mathbf{H}_f^{(i)} - \nabla Q(\mathbf{H}_f^{(i)})/L_f\right)$;
  $i = i + 1$;
until *convergence*;

IV. Experiments

In this section, we evaluate the proposed algorithms. The TLS reconstruction method is used as the reference baseline.

We use a GW signal of an equal-mass non-spinning black-hole binary with total mass 50 $M_\odot$ at a sample rate of 4096 Hz. [1].

We choose to place the source at an arbitrary position in the sky corresponding to RA $= 82.59°$, dec $= 54.31°$ at GPS time 1187007042 (Thu Aug 17 12:10:24 GMT 2017). This source direction leads to the beam pattern matrix as follows [2]:

$$\mathcal{F} = \begin{pmatrix} 0.8402 & -0.0712 \\ -0.8223 & 0.2813 \\ -0.1199 & 0.6785 \end{pmatrix}. \tag{11}$$

We intentionally choose this beam pattern matrix which avoids the rank deficiency problem [5]. We manually decreased the noise in Virgo by a factor of 3 in order to enhance the SNR fraction brought by the $\times$ polarization, and be more representative of future science runs. The input SNR [1] varies from ~ 24 to ~ 240.

We compare between the TLS method in (6) and the proposed sparsity-based algorithms with Lasso (8) and WGL (9) shrinkage operators. The methods are compared against their relative reconstruction error (RRE), classically used as a figure-of-merit:

$$\text{RRE} = \frac{\|\mathbf{H} - \hat{\mathbf{H}}\|_F^2}{\|\mathbf{H}\|_F^2}, \tag{12}$$

where $\hat{\mathbf{H}}$ is the estimated polarizations in the matrix form.

The reconstruction level of all the presented methods depends on the thresholding chosen in the algorithms. Therefore, we test several values for the threshold and then select the one which corresponds to the best performance. For the proposed algorithms, we use the same threshold for all frequencies for the sake of simplicity. Although such an oracle is not possible in practice, it allows a best-case comparison of the different methods. We also show the performance of the presented algorithms as a function of the sparsity level of the estimation.

[1]We used the software package LALSuite https://wiki.ligo.org/DASWG/LALSuite

[2]The order from top to bottom is LIGO Hanford, LIGO Livingston and Virgo.

Fig. 1 shows the performance as a function of the input SNR. The neighborhood in these experiments for WGL is chosen to be horizontal and equal-weighted which promotes the clustering effect in the time direction. The size of the neighborhood is fixed to 5 time-frequency pixels. We also tested different sizes, and neighborhood in the vertical direction, and find out similar performances. We may investigate neighborhoods that are adapted to typical frequency evolution (horizontal for the early/low-frequency part of the signal where the frequency varies slowly and vertical for the later/high-frequency part of the signal close to the final merger). The reconstruction is performed with 10 different noise realizations. The mean RRE and error bars are shown in the figure. The considered methods of TLS, Lasso and WGL shows comparable RRE for the considered range of input SNR.

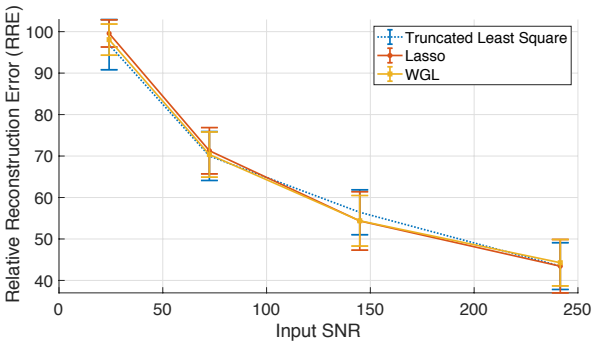

Fig. 1. Reconstruction performance *vs* input SNR. The mean value and 1-sigma error bars obtained over 10 noise realizations are shown.

However, the reconstructions from the various methods differ significantly and the RRE figure-of-merit does not capture that difference. In Fig. 2 we show the performance of TLS and WGL for one noise realization as a function of the sparsity level [3] of the estimation for different input SNR.

At the minimum RRE working point, the WGL method selects more pixels than the TLS method. We illustrate this in Fig. 3 by using a representative example of our simulations. We show the whitened noisy observations and the whitened noise-free detector responses for an input SNR of ~ 72. The injected signal is relatively strong in the two LIGO detectors and is contaminated by relatively larger noise in Virgo. This is due to the specific position of the sky we selected and the sensitivity difference in detectors.

Fig. 4 shows the estimated polarization waveforms along with the original polarizations for the WGL and TLS algorithms, using a threshold that corresponds to the best RRE.

We see that $h_+(t)$ is much better reconstructed by both algorithms, and this is due to the larger sensitivity of the detector network from that polarization as explained above.

The WGL algorithm restores a much larger fraction of the "+" polarization (till $t > 0.9$ s) than the TLS algoritm. It thus allows for a more complete reconstruction of the signal

[3]We define the sparsity level as the percentage of the number of zero elements in the vector. A higher value means sparser result.

ISBN 978-90-827970-1-5 © EURASIP 2018

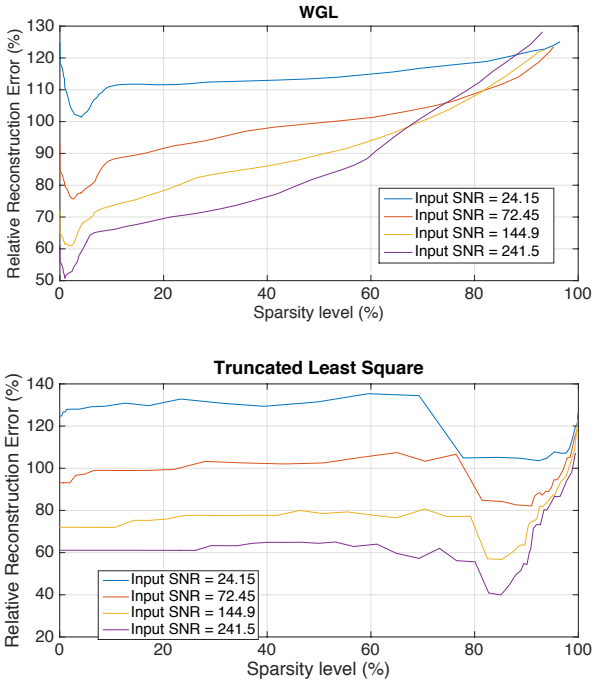

Fig. 2. Reconstruction performance *vs* sparsity level of the estimation for Windowed Group Lasso (WGL) algorithm (top) and the Truncated Least Square (TLS) algorithm (bottom). The two algorithms end up making a very different pixel selection at the best relative reconstruction error (RRE). The WGL method selects more pixels than the TLS method.

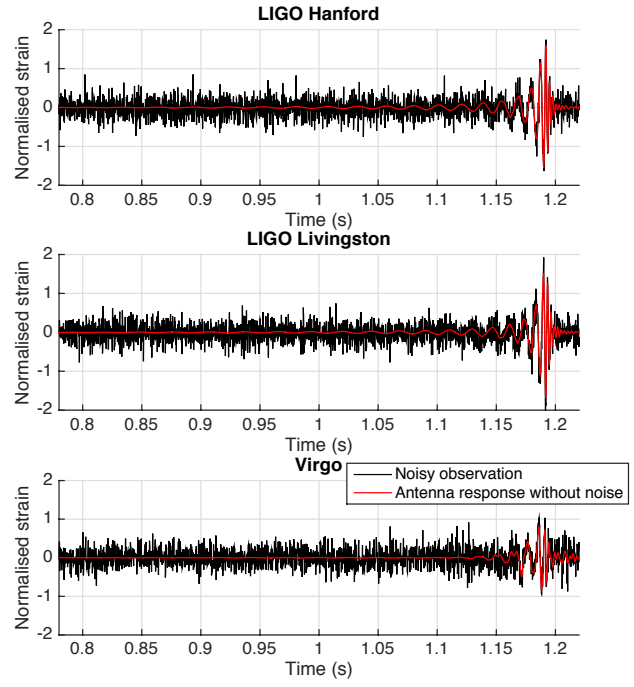

Fig. 3. Whitened observations in the detectors and the whitened antenna response without noise.

at lower frequencies. This is performed at the price of a small noise residual.

This is clearly seen in Fig. 5 that presents the associated spectrograms obtained with the WGL and TLS algorithms, where the low-frequency part of waveform appears to be missing in the TLS reconstruction.

The reliable estimate of the low-frequency part of the incoming GW polarizations may have direct implications for the astrophysical interpretation of the observations, e.g., to test whether the orbital motion of the source is precessing [2].

V. Conclusion

In this article, we proposed a new approach for the reconstruction of the GW polarizations from the noisy observations based on sparsity regularization. We show that promoting the time-frequency sparsity helps reduce the reconstruction error where the signal goes closer to or below the noise level. We adapted the reconstruction algorithm based on "structured sparsity" introduced in [21] to the case of additive colored noise. This algorithm provides a promising result in our tests. For now, we have only tested this idea with rather crude and generic neighborhoods. We expect better results when using neighborhood shapes motivated by astrophysical models.

Acknowledgments

This research was supported by the French Agence Nationale de la Recherche (ANR) under reference ANR-15-CE23-0016 (Wavegraph project).

References

[1] B. Sathyaprakash and B. F. Schutz, "Physics, astrophysics and cosmology with gravitational waves," *Living Rev. Rel.*, vol. 12, no. 1, p. 2, 2009.

[2] J. Flamant, P. Chainais, E. Chassande-Mottin, F. Feng, and N. Le Bihan, "Non-parametric characterization of gravitational-wave polarizations," This volume, 2018.

[3] S. Klimenko *et al.*, "Constraint likelihood analysis for a network of gravitational wave detectors," *Phys. Rev. D*, vol. 72, no. 12, p. 122002, 2005.

[4] S. D. Mohanty *et al.*, "Variability of signal-to-noise ratio and the network analysis of gravitational wave burst signals," *Class. Quantum Grav.*, vol. 23, no. 15, p. 4799, 2006.

[5] M. Rakhmanov, "Rank deficiency and Tikhonov regularization in the inverse problem for gravitational-wave bursts," *Class. Quantum Grav.*, vol. 23, no. 19, p. S673, 2006.

[6] S. Klimenko *et al.*, "Method for detection and reconstruction of gravitational wave transients with networks of advanced detectors," *Phys. Rev. D*, vol. 93, no. 4, p. 042004, 2016.

[7] N. J. Cornish and T. B. Littenberg, "BayesWave: Bayesian Inference for Gravitational Wave Bursts and Instrument Glitches," *Class. Quantum Grav.*, vol. 32, no. 13, p. 135012, 2015.

[8] I. Di Palma and M. Drago, "Estimation of the gravitational wave polarizations from a nontemplate search," *Phys. Rev. D*, vol. 97, no. 2, p. 023011, Jan. 2018.

[9] H. W. Engl, M. Hanke, and A. Neubauer, *Regularization of inverse problems*. Springer Science & Business Media, 1996, vol. 375.

[10] M. Kowalski, "Sparse regression using mixed norms," *Appl. Comp. Harm. Anal.*, vol. 37, no. 3, pp. 303–324, 2009.

[11] A. Torres-Forné *et al.*, "Denoising of gravitational wave signals via dictionary learning algorithms," *Phys. Rev. D*, vol. 94, no. 12, p. 124040, 2016.

[12] P. Addesso *et al.*, "Sparsifying time-frequency distributions for gravitational wave data analysis," in *Proceedings 3rd IEEE CoSeRa workshop*, 2015, pp. 154–158.

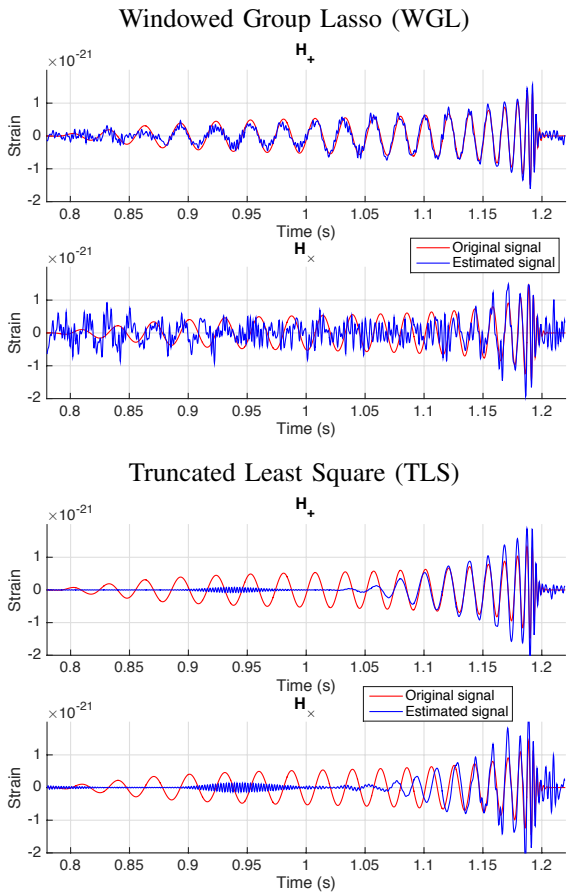

Fig. 4. Original (red) and estimated (blue) polarization waveforms associated with the observations of Fig. 3. The estimation is performed with the Windowed Group Lasso (WGL) algorithm (top) leading to a Relative Reconstruction Error (RRE) of 75.64%, and with the Truncated Least Square (TLS) algorithm (bottom) with a RRE of 82.31%.

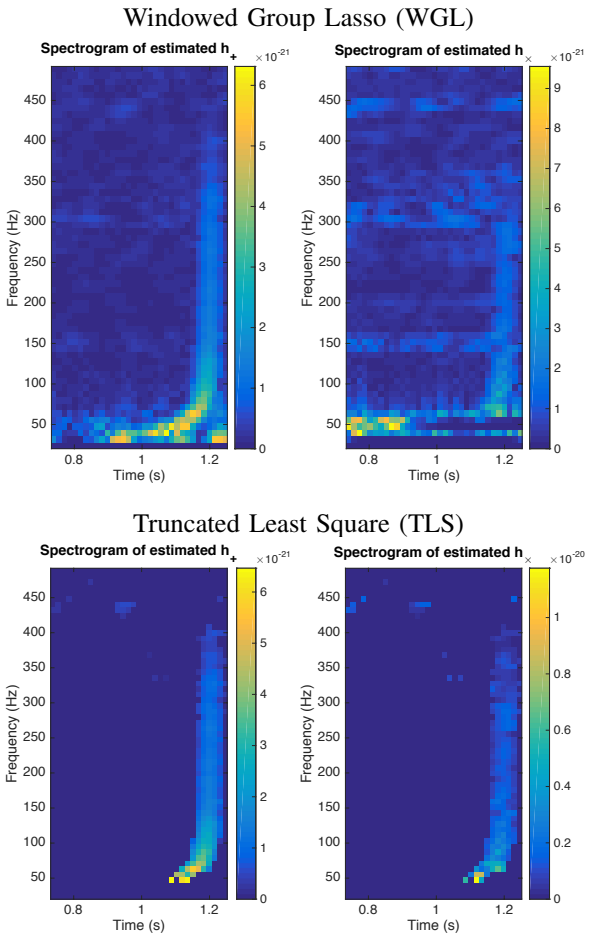

Fig. 5. Spectrograms of the estimated polarization waveform shown in Fig. 4 with Windowed Group Lasso (WGL) algorithm (top) using a 5-pixel neighborhood in the time direction leading to a sparsity level of 2.54%; and with the Truncated Least Square (TLS) algorithm leading to a sparsity level of 89.87%.

[13] B. Abbott *et al.*, "Multi-messenger observations of a binary neutron star merger," *ApJ Lett.*, vol. 848, no. 2, p. L12, 2017.

[14] P. L. Sondergaard, B. Torresani, and P. Balazs, "The linear time frequency analysis toolbox," *International Journal of Wavelets, Multiresolution and Information Processing*, vol. 10, no. 04, 2012.

[15] S. Klimenko *et al.*, "Method for detection and reconstruction of gravitational wave transients with networks of advanced detectors," *Phys. Rev. D*, vol. 93, no. 4, p. 042004, 2016.

[16] S. Mallat, *A wavelet tour of signal processing: the Sparse way*, 3rd ed. Burlington, MA: Academic Press, 2009.

[17] R. Tibshirani, "Regression shrinkage and selection via the LASSO," *J. Royal Stat. Soc. B*, pp. 267–288, 1996.

[18] P. L. Combettes and J.-C. Pesquet, "Proximal splitting methods in signal processing," in *Fixed-point algorithms for inverse problems in science and engineering*. Springer, 2011, pp. 185–212.

[19] K. Siedenburg, M. Kowalski, and M. Dörfler, "Audio declipping with social sparsity," in *Proceedings ICASSP*, 2014, pp. 1577–1581.

[20] F. Feng and M. Kowalski, "Hybrid model and structured sparsity for under-determined convolutive audio source separation," in *Proceedings ICASSP*, 2014.

[21] M. Kowalski, K. Siedenburg, and M. Dörfler, "Social sparsity! neighborhood systems enrich structured shrinkage operators," *IEEE Trans. Signal Proc.*, vol. 61, no. 10, pp. 2498–2511, 2013.

ISBN 978-90-827970-1-5 © EURASIP 2018